Ionospheric Science at the Reagan Test Site

Stephen M. Hunt, Frederick J. Rich, and Gregory P. Ginet

The Reagan Test Site is located just north of the geomagnetic equator below one of the most complex regions of Earth's ionosphere. For nearly 50 years, the site's advanced radar technology and precise measurement techniques have provided comprehensive data on the physical properties of the equatorial ionosphere and radio-wave signal propagation effects.

The high-power, large-aperture radar systems at the Reagan Test Site (RTS) on the Kwajalein Atoll transmit signals at frequencies spanning 150 MHz to 35 GHz to track satellites, ballistic missile components, and airborne calibration targets [1]. The ionosphere extends from about 90 to 2000 km altitude and modifies the propagation path of these radar signals in a frequency-dependent manner. Downward-transmitting, spaceborne radio-frequency (RF) systems are similarly impacted. Radar measurement parameters adversely affected by the ionosphere include target position, velocity, and radar cross-section accuracy. Figure 1 illustrates the typical frequency-dependent (ultra-high frequency [UHF], very high frequency [VHF], and L band) impact of ionospheric radar range bias experienced at RTS as a function of elevation angle. The ionospheric range biases shown here are proportional to the integrated electron density (the total electron content [TEC]) along the signal path. Currently, RTS uses the real-time ionospheric error-correction model (IECM) to compensate for the effects of atmospheric and ionospheric biases on radar data [2].

The broad set of mission areas at RTS, and the associated demand for improved radar capabilities required to meet mission needs, has driven five decades of ground-breaking work to forward the state of the possible in ionospheric science and engineering. RTS's location very close to the geomagnetic equator (4° north geomagnetic latitude) and its radar systems that operate at frequencies spanning from the VHF to Ka band regimes have led to extremely challenging ionospheric characterization and modeling problems. Through the

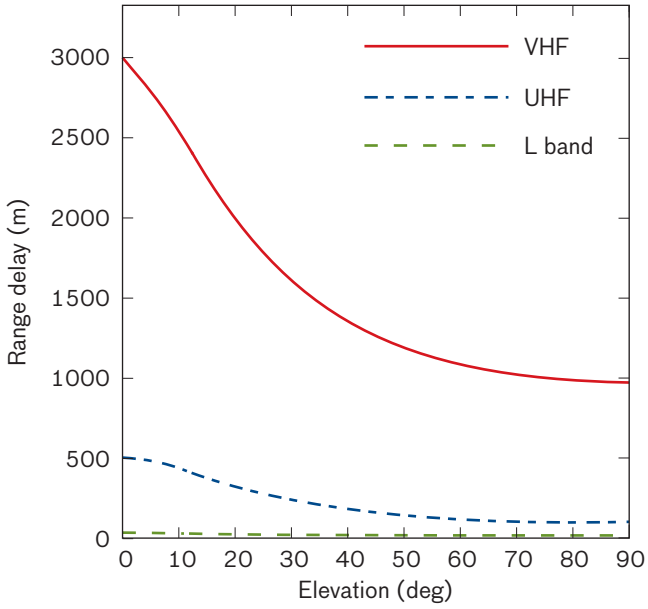

FIGURE 1. The ionospheric range delay is computed by using the RTS empirical elevation mapping function. This plot was created for ionospheric conditions with a vertical total electron content (TEC, in units of 10^{16} electrons/m^2) value of 65.3, or a one-way VHF range delay of 1.0 km. These conditions are consistent with moderate solar activity. This function maps the vertical line-of-sight TEC value to an arbitrary elevation angle. It is derived from historic multifrequency missile data collected at RTS. This figure also illustrates the frequency-dependent (~$1/f^2$) signal propagation (range delay) effects at VHF (red curve), UHF (blue dashed curve), and L band (green dashed curve).

decades, Kwajalein has become populated with a comprehensive suite of complementary ionospheric measurement systems, such as an all-sky imager, U.S. Air Force Global Positioning System (GPS) receivers, and a vertical ionospheric sounder. An incoherent scatter radar measurement capability is in place at the Advanced Research Projects Agency (ARPA) Long-Range Tracking and Instrumentation Radar (ALTAIR) system. RTS's highly calibrated equatorial ionospheric data are highly sought after by both Department of Defense (DoD) and academic scientific communities. These data are used to guide solutions to ionospheric impacts on ground- and spaced-based systems (Table 1).

The Future of Ionospheric Science at RTS

RTS has enjoyed 50 years of investment and upgrades in RF measurement equipment that, in part, supports atmospheric and ionospheric study. In the future, it is expected that RTS will continue its contributions to a better understanding of the complexities of the equatorial ionosphere.

The inversion process of determining ionospheric properties—such as TEC and electron volume density at a specific time and location—from RF measurements depends on the quality (accuracy and precision) of the radar data. The collection, analysis, and fusion of these radar data with the complementary ionospheric parameters measured by other systems at RTS will enable an

Table 1. Potential impacts caused by ionospheric effects

Asset	Impact
Radar	Satellite position and radar-cross-section errors
GPS	Tracking and signal degradation
Satellite communications	Communication link degradation
Radio communications	Radio blackout
Satellite signals intelligence (SIGINT)	Geolocation error
Low-Earth-orbit satellites	Enhanced drag Inaccurate space situational awareness

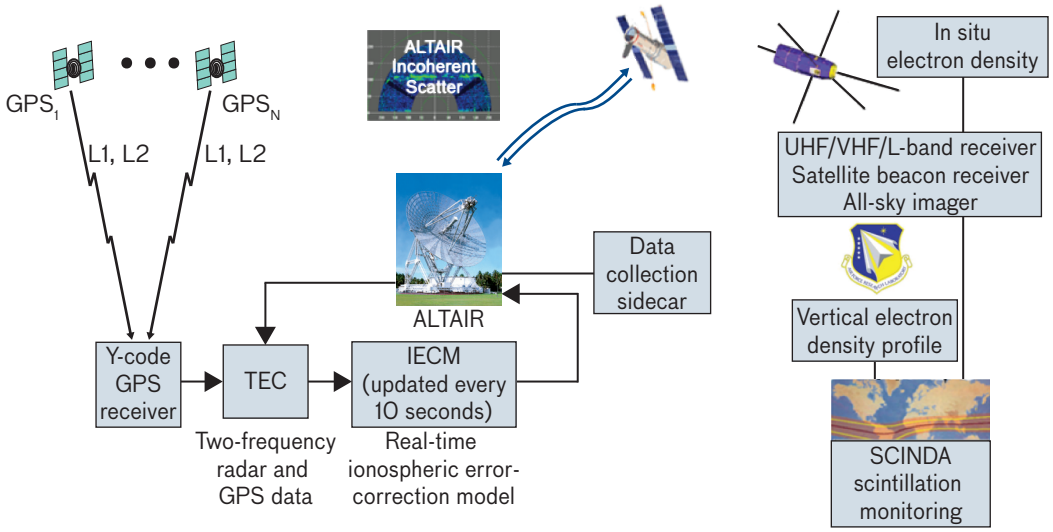

FIGURE 2. The RTS Space Weather Testbed concept provides a comprehensive suite of ionospheric data-collection hardware and real-time modeling tools. These tools and data can provide significantly improved real-time modeling accuracy and a posteriori analysis of fused ionospheric data from RTS measurement systems. As illustrated above, the inclusion of in situ satellite data and its fusion with ground-based measurements can enhance detailed analysis of spacecraft interactions. Highly accurate measurements from RTS systems have a long history of providing fundamental data to support national programs.

improved understanding of transient ionospheric effects and, in turn, will aid radar accuracy improvements.

Several complementary measurement systems located on Roi-Namur Island will, once integrated, provide enhanced ionospheric characterization through data fusion (Figure 2). Table 2 contains an overview of RTS measurement systems and the physical parameters that they provide, or could provide, to support radar accuracy improvements and global ionospheric specification. The data fusion can incorporate measurements from the ionospheric sounder on Roi-Namur, incoherent scatter radar data from ALTAIR, GPS TEC, and ALTAIR TEC. New cross-calibration, interpolation, and physics-based modeling algorithms will be required. To support this effort, the ionospheric measurement systems at RTS will need to be upgraded and expanded; for example, the 12-year-old Y-code receiver should be updated to accommodate U.S. Air Force GPS as well as Russian Global Navigation Satellite System (GLONASS) data. Implementation of a net-centric ionospheric data capability would also allow RTS to publish parameters for regional application within the DoD and for integration with a global ionospheric reference model. The characterization of ionospheric properties obtained from these measurements will aid in achieving improved accuracies for RTS radar and other national systems.

Properties of Earth's Ionosphere

Starting above the mesosphere at ~80 km altitude, the near-Earth space environment comprises the thermosphere, the ionosphere, and the magnetosphere [3]. Similar to the familiar tropospheric weather, dynamic phenomena in these regions (often called space weather) are driven by the sun [4]. The physical mechanisms, however, are quite different. Figure 3 summarizes the solar drivers of space weather and the resultant environmental effects at Earth. For completeness, the broad range of space-weather phenomena is shown in Figure 3. This article focuses on the ionosphere and its relationship to RTS radar and ionospheric measurement systems.

As the altitude above the Earth increases, the density of the atmosphere decreases exponentially. At its outer limit, atmospheric gases diffuse into interplanetary space. The first 90 km of the atmosphere consist of a mixture of neutral gases with weak ionization. The troposphere (the atmospheric "layer" up to 15 km above the Earth's surface) is mixed by turbulence, which is primarily the result of thermal winds coupled with forces from the Earth's rotation. Above an altitude of approximately 90 km, the gases are ionized by solar extreme ultraviolet (EUV) radiation and form the ionosphere (Figure 4).

Table 2. RTS measurement systems

Instrument	System data	Ionospheric physical parameters	Role
ALTAIR and TRADEX	Scintillation index from amplitude vs. time series	Irregularity detection and location	Characterize transient effects
Ionospheric sounder	Maximum usable frequency Time delay	Electron density vs. height (height to peak, plus more)	Calibrate incoherent scatter radar (ISR) data and IECM
ALTAIR	Group delay at UHF and VHF	Line-of-sight total electron content	Calibrate GPS receiver Input for IECM Real-time ionospheric correction
ALTAIR	Power vs. range, azimuth, and elevation (incoherent scatter)	Line-of-sight electron volume density	Input for IECM
Y-code GSP receiver	Group delay and phase advance at L1 and L2	Line-of-sight total electron content Irregularity detection	Input for IECM Characterize transient effects
Scintillation Network Decision Aid (SCINDA)	Scintillation index from amplitude vs. time data	Irregularity detection and location (map)	Transient effect identification and warning
Neutral atmosphere			
All-sky imager	Image intensity vs. location	O+ emission detection (green)	Optical background brightness detection
RTS weather station			
Balloon-borne radiosonde	Pressure, temperature, position (altitude), wind (velocity), relative humidity		Post-mission reentry data calibration Neutral density index of refraction

Free electrons and ions are present in nearly equal numbers in the ionosphere, resulting in an overall net neutral charge for the particle distribution. Recombination of the ionized particles proceeds slowly enough to allow high concentrations of free electrons to persist even throughout the night. These concentrations on both the day and night side are more intense during periods of moderate to high solar activity. During the daytime, as shown in Figure 4, several distinct layers are formed (called regions D, E, and F). Each region is created by a balance between photoionization and recombination based on the chemistry of the neutral atmosphere at each altitude [5]. The names of the layers are derived from the fact that the first layer discovered was called the "electric" layer or E layer. At nighttime, recombination dominates, and the layers often merge into a single region with reduced electron density.

The distribution and dynamics of these ionized particles are governed by the solar flux distribution, the Earth's magnetic field, interactions with the neutral atmosphere, and space weather. Effects of the latter include enhanced collisional ionization, Joule heating, and plasma transport caused by large- and small-scale electric fields. All these effects can dramatically alter the electron density and change the location of the peak and the shape of the ionospheric layers. In addition to natural space-weather variations, high-altitude nuclear detonations also gave rise to large ionospheric effects in the Pacific region near RTS during the early 1960s [6]. In particular, the Starfish detonation on 9 July 1962 occurred in the F region (400 km altitude) and caused significant enhancement in trapped charged particles with induced aurora. This enhancement affected high-frequency (HF) communications and persisted for weeks in the F region.

Space weather and the Earth's strong magnetic field relative to any induced magnetic field have dominant influences on the dynamical aspects of the ionosphere. The distribution of incident solar EUV radiation and the

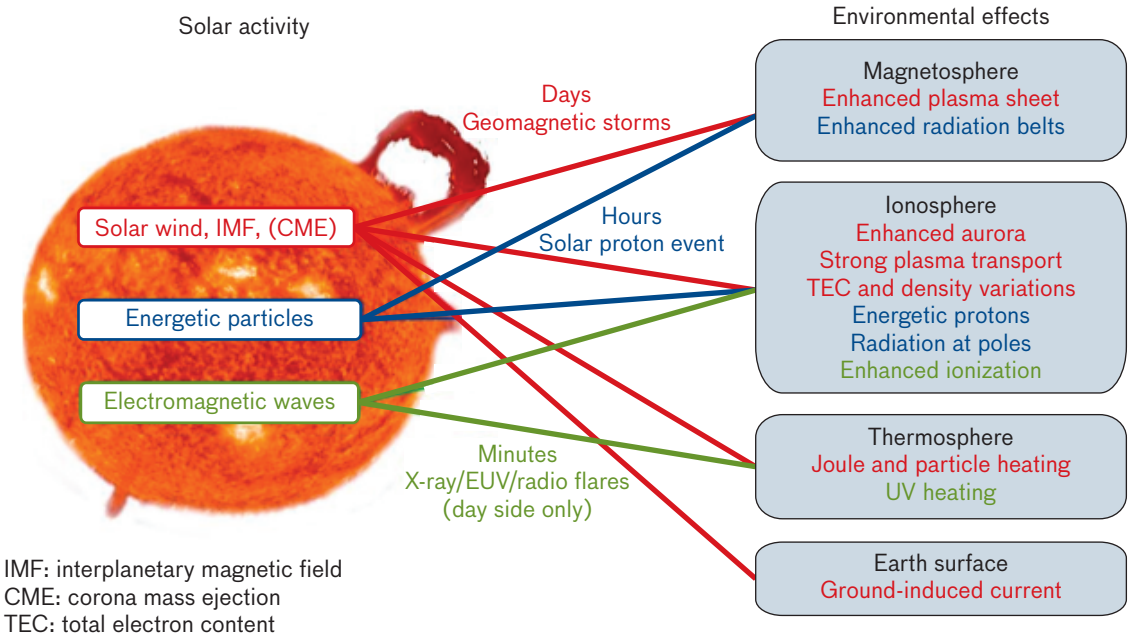

FIGURE 3. This illustration highlights the sun-Earth impacts on Earth's magnetosphere, ionosphere, thermosphere, and surface. The solar wind, energetic particles, and electromagnetic waves all significantly affect the distribution and dynamics of atmospheric ionization at different timescales (days, hours, and minutes).

latitudinal variation of Earth's magnetic field naturally divide the ionosphere into three characteristic latitudinal zones of distinct physical structure: polar, midlatitude, and equatorial. At radio wavelengths, signal propagation in these regions is governed by an index of refraction that changes with the variations in electron density. Consequently, the speed and direction of RF waves change as the waves pass through the ionosphere. The radar measurements made by RTS systems of objects within or above the equatorial ionosphere are correspondingly changed, and the variations can affect radar mission performance [7].

Properties of the Equatorial Ionosphere

In the daytime equatorial ionosphere, electron density enhancements form near 15° to 20° north and south latitude. The equatorial anomaly is the electron-density depletion region that forms near the geomagnetic equator directly above RTS [8]. Figure 5 illustrates the equatorial anomaly as observed from RTS in the reference frame of the radar system. This distribution is caused by the vertical electrodynamic drift of the plasma at the equator and

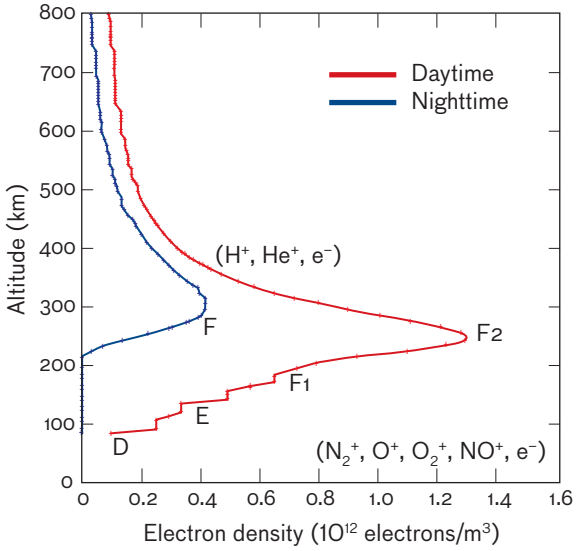

FIGURE 4. Daytime and nighttime electron density distributions of Earth's ionosphere as a function of altitude illustrate how the ionosphere appears during undisturbed periods. The blue curve shows the significant reduction in electron density during the evening hours. The red curve shows the different ionospheric regions that form during the daytime as a result of ionization caused by incident solar radiation.

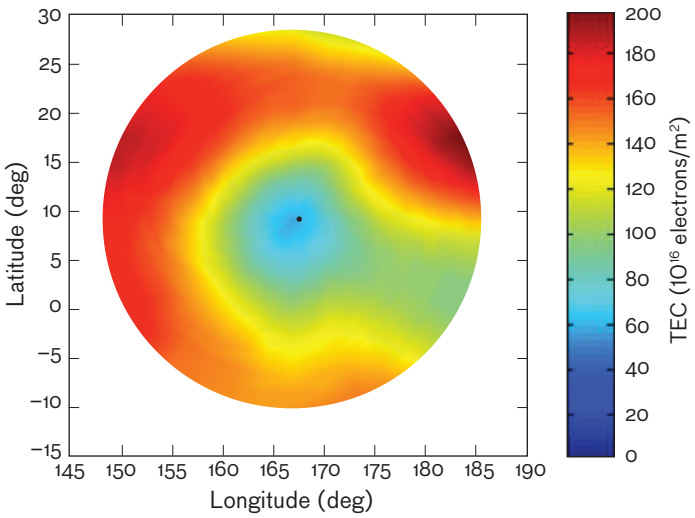

FIGURE 5. The plot contains the total electron content (TEC), computed by the ionospheric error-correction model (IECM), along the radar line of sight to an altitude of 400 km. This distribution is how the equatorial ionosphere appears in the reference frame of the RTS radar systems. Note the electron density depletion forming along the geomagnetic equator directly above RTS. This characteristic depletion region (equatorial anomaly) forms daily and is governed by the physics of the equatorial ionosphere. These data were collected during a period of increased space-weather activity, the July 2000 Bastille Day solar storm that occurred near the peak of solar cycle 23. The westerly density enhancement is due to the daily movement of incident solar radiation with time. Under normal conditions, this distribution tends toward an equilibrium state during the late evening to early morning hours. The location of RTS (8.72° N and 167.73° E) is marked with the small black dot.

its later diffusion along the north-south geomagnetic field lines (B). An east-west–oriented electric field (E) at the geomagnetic equator perpendicular to the north-south magnetic field causes this vertical E × B (force) drift. When the plasma reaches an altitude at which the ion-neutral collision frequency is low, the plasma diffuses downward along the north-south geomagnetic field lines to higher and lower latitudes.

As the ionosphere and thermosphere cool after sunset, neutral gas descends in altitude, but the ionized gas becomes trapped because it cannot travel perpendicular to Earth's magnetic field because of magnetic forces. (Earth's magnetic field is nearly parallel to the surface of the Earth at the equator.) This trapped gas can lead to an electrodynamic Rayleigh-Taylor type instability in which forces with sufficient strength eventually drive the ionized gas motion in a chaotic manner. Low-density (warmer) electron-density regions on the bottom of the ionosphere drift upward into higher-density (cooler) regions as plumes and bubbles (also called ionization depletion regions). Starting at large scales (~100 km in the east-west direction), the instability cascades to small scales (~100 m) to form irregularities that cause signal scintillation and frequency spreading (equatorial spread F) of VHF and UHF radar signals. These irregularities can persist in the F region during the early evening to early morning hours.

Transionosphere Radar Wave Propagation

Radio-frequency signal-propagation effects depend on the index of refraction along the signal path between the transmitter and receiver. The index of refraction, n, is modeled from the physical properties and distribution of the neutral atmosphere and the ionosphere. Its value and form literally change with the weather on extremely short and long timescales as well as on small- and large-length scales. The neutral atmospheric index of refraction is nondispersive, i.e., it does not depend on frequency but does depend strongly on the atmospheric pressure, temperature, and relative humidity along the signal-propagation path [9].

In contrast, the index of refraction in the ionosphere is dispersive and is strongly dependent on electron density. Edward Appleton, the 1947 Nobel Prize winner in physics, derived an equation (see sidebar) for the ionospheric index of refraction, assuming a cold plasma. In RF applications such as GPS and RTS radar, the signal angular frequency ω is much greater than the electron density-dependent plasma frequency ω_p (see sidebar for symbol definitions), and magnetic field effects are small. For these RF applications , the Appleton-Hartree relation can be simplified to $n = \sqrt{(1-\omega_p^2/\omega^2)}$ and is applied for real-time modeling with mostly satisfactory results [10]. Collisions have been neglected, and magnetic field effects are not calculated for the limiting case $\omega \rightarrow \infty$, where the vacuum solution $n = 1$ is recovered.

Appleton-Hartree Equation

The Appleton-Hartree equation [11] for the refractive index n that governs the propagation of an electromagnetic wave of angular frequency $\omega = 2\pi f$ (where f is the frequency in Hz) in a cold, magnetized plasma is given by

$$n^2 = 1 - \frac{X}{1 - jZ - \frac{\frac{1}{2}Y^2\sin^2\delta}{1 - X - jZ} \pm \frac{1}{1 - X - jZ}\left(\frac{1}{4}Y^2\sin^2\delta + Y^2\cos^2\delta(1 - X - iZ)^2\right)^{\frac{1}{2}}}$$

where $X = \omega_p{}^2/\omega^2$, $Y = \omega_H/\omega$, $Z = \nu/\omega$, with

$\omega_H = \frac{B_0|e|}{m}$ = the cyclotron frequency, $\omega_p = \sqrt{\frac{Ne^2}{\varepsilon_0 m}}$ = the plasma frequency,

and ν = the collision frequency, B_0 = the magnitude of the Earth's magnetic field, δ = the angle between the magnetic field and the wave vector, N = the electron density, m = the electron mass, e = the electron charge, ε_0 = the permittivity of free space and $j = \sqrt{-1}$.

There are two solutions to the Appleton-Hartree equation, depending on the choice of sign (±) in the denominator. Known as the fast and slow modes, also called the "ordinary" (O) and "extraordinary" (X) modes if the wave vector is oriented predominantly perpendicular to the background magnetic field, these waves exhibit a wide variety of behaviors as a function of plasma density, magnetic field strength, and wave-vector orientation. Effects include wave resonances, propagation cutoffs, and changing polarizations. A striking example of the different propagation behaviors of the two modes can be found for certain wave parameter values in the high-frequency (HF) radar regime where $\omega \geq \omega_p$. When launched at the same frequency, angle, and location, the O mode can escape the ionosphere entirely while the X mode becomes trapped in the Earth-ionosphere waveguide, as illustrated by the ray-tracing example in Figure A.

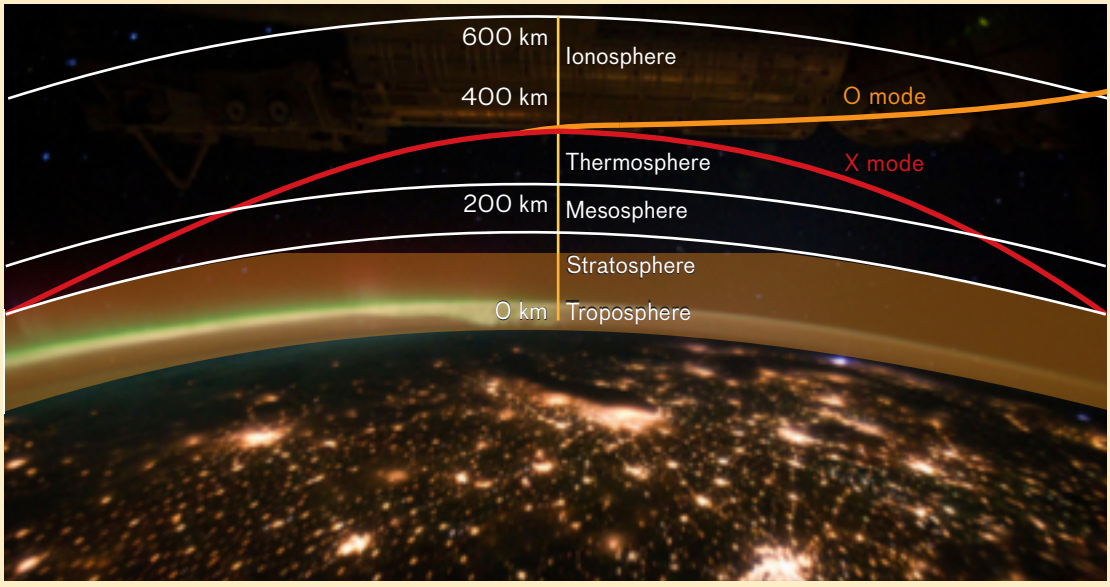

FIGURE A. The numerical ray trace of a high-frequency wave in a model ionosphere shows the splitting of O and X modes, with the O mode punching through the ionosphere and the X mode bending back.

Radio-frequency signal-propagation effects resulting from the inhomogeneous, non-isotropic ionosphere include elevation-angle bending, range delay, Doppler frequency shifts, polarization rotation, and frequency spreading. In addition, if the inhomogeneity is changing rapidly enough because of ionosphere dynamics, then signal amplitude and phase scintillation can occur. These effects degrade radar system measurement accuracy. Because radar systems collect position, velocity, and radar cross-section data on objects that traverse the troposphere (the lower atmosphere) and the ionosphere (region above 90 km), researchers have spent many years developing spatially dependent and time-dependent RF signal-propagation models to mitigate adverse effects on signals. Given the often dynamic nature of the atmosphere and ionosphere, it is effectively impossible to predict propagation effects without the aid of real-time measurements of the physical properties that govern the index of refraction. These models consist of two main components: (1) the spatially varying and time-varying properties of the index of refraction in each region of the atmosphere and ionosphere, and (2) the corresponding RF signal-propagation effects.

The index of refraction is calculated, and its distribution is often modeled by using the stratified layer method. This distribution model is used for frequency-dependent ray tracing (see Figure 6). Finally, the time delay and elevation-angle bending at each boundary in the ray trace is summed to determine total refraction values. The success or failure of any particular modeling approach depends on the accuracy of the measured results for the target location. Over the past 35 years, real-time modeling techniques have evolved by exploiting increased computational capacity and the increasing number of ionospheric measurement systems.

Early Ionospheric Radio Research

Ionospheric radio-signal characterization at Lincoln Laboratory has its origins in the 1950s in support of long-wavelength military communications and DoD research. During this period, the Lincoln Laboratory Radio Physics Division collaborated on the science of vertical ionospheric sounders. These systems aided Army Signal Corps activities by providing bottomside ionospheric parameters. Sounders provide physical parameters that enable long-distance, long-wavelength communications. The long-wavelength radio research with the Army Signal Corps led to the Kwajalein-based, long-wavelength communication facility. In more recent years, digital sounders have been distributed globally to support scientific study and to drive ionospheric models with measurement updates of the vertical electron density. One such sounder, built by the University of Massachusetts–Lowell and funded by the Air Force Research Laboratory, is operating on Roi-Namur (Figure 7) [12]. The RTS ionospheric sounder is used to calibrate ALTAIR incoherent scatter radar measurements and to measure the bottomside ionospheric component of space-weather phenomena.

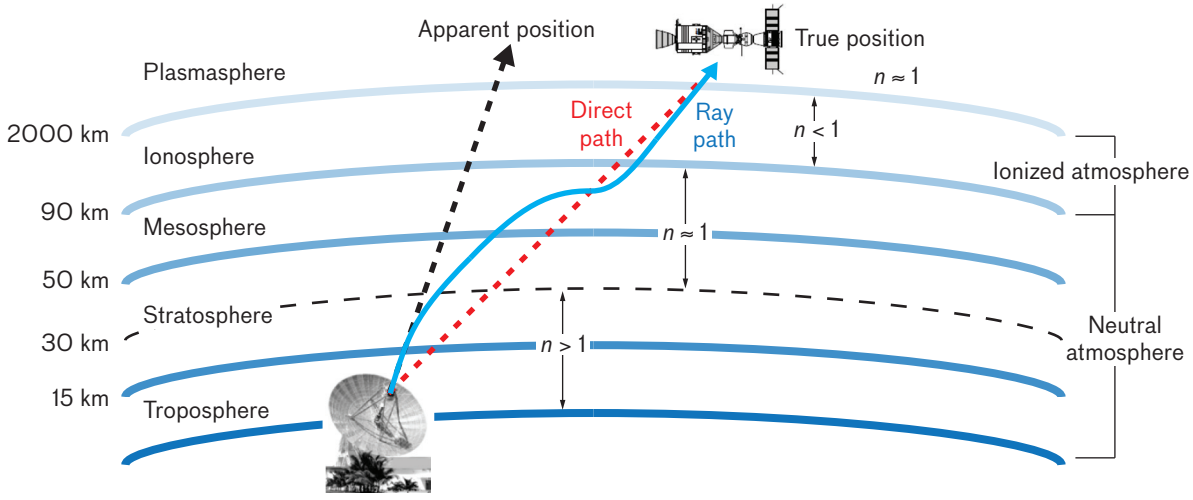

FIGURE 6. RF signals are transmitted from the Earth's surface through the neutral and ionized atmosphere. A ray-tracing algorithm computes range and elevation-angle biases derived from the altitude-dependent index of refraction n to accurately determine satellite position. Note the vertical scale is not linear.

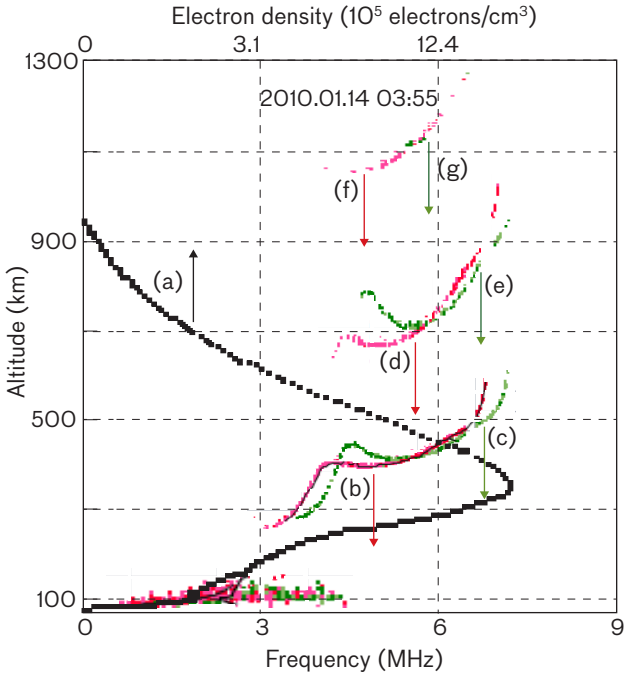

FIGURE 7. These RTS vertical sounder data collected on Roi-Namur support the Air Force Research Laboratory Scintillation Network Decision Aid (SCINDA) network. The University of Massachusetts–Lowell digisonde provides regular measurements of the vertical electron density as a function of true height. The black curve (a) is the electron number density (nonlinear *x*-scale at top of figure) computed by the RTS digisonde system versus true altitude. These are the data of most interest for RTS applications. The red curve (b) and the green curve (c) are ordinary and extraordinary signal returns (*x*-scale at bottom of figure) versus their corresponding apparent altitude, respectively. Curves (d) through (g) are the corresponding double-hop and triple-hop signal returns for the ordinary and extraordinary modes. A detailed description of all sounder returns is beyond the scope of this article but can be found in the G. Williams reference [13].

In 1952, German scientist Winfried Otto Schumann hypothesized the existence of an extremely-low-frequency (ELF) radio-resonance propagation effect that could occur in Earth's ionospheric cavity [14, 15]. Lightning strikes provide power that generates a standing wave mode in the atmospheric waveguide bounded on the bottom by the conducting Earth and on the top by the conducting ionosphere. This effect caught the interest of Lincoln Laboratory researchers Martin Balser and Charles Wagner [16]. Their measurements and analysis using laboratory low-frequency sounding hardware proved the hypothesized propagation effect proposed by Schumann (Figure 8). A Lincoln Laboratory academic collaboration also helped researchers at The Ohio State University by supporting the collection of state-of-the-art ionospheric sounding data during the International Geophysical Year of 1958 [17]. During the early 1960s, Donald Farley of Cornell University published a series of papers on the incoherent scatter radar method [18]. These papers described the relationship between radio-signal returns from ionospheric electrons (plasma) and the physical properties (electron density and location) of the plasma itself. One very important implication of this work is that radar refraction effects from the ionosphere can be obtained directly from backscatter data [19]. This finding could greatly simplify present-day modeling architectures in use by radar systems. In recent years, RTS has gained the unique suite of capabilities to develop and validate this method for operational use.

During the 1960s and 1970s, RTS was growing with the addition of the Target Resolution and Discrimination Experiment (TRADEX) radar (L band and S band) and ALTAIR (UHF and VHF) systems on the island of Roi-Namur. The ALTAIR real-time system requirements were published in 1965, and the radar's initial operating capability began in 1970. At this time, the ALTAIR simultaneous detection capability (UHF and VHF) did not include real-time ionospheric compensation. The advantage of the lower-frequency ALTAIR system is that it provides a larger angular search region for the acquisition of a target complex. At ALTAIR, the UHF and VHF half-power beamwidths are 1.1° and 2.8°, respectively. For TRADEX, the L-band half-power beamwidth is 0.6°. The downside of lower operating frequencies is the presence of greater biases and signal pulse distortion caused by ionospheric dispersion. In the early 1970s, Theodore Pass, a researcher from Lincoln Laboratory, characterized tracking data collected on known targets and demonstrated that atmospheric and ionospheric refraction biases constrained the achievable accuracy limit for the Kwajalein radar systems.

History of RTS Modeling of the Ionosphere

During the 1960s and early 1970s, RTS efforts sought to improve radar accuracy by modeling the atmospheric and ionospheric measurement biases. The neutral atmosphere (below 90 km) was modeled first and the ionosphere (90 km to 2000 km) later. The RTS models are primarily focused on correcting for the effects responsible for radar-range bias (time delay), elevation-angle bias, and radar transmit pulse dispersion.

The need to search, track, and collect highly accurate target data and to achieve real-time integration of the Kwajalein radar systems drove the early refraction bias modeling efforts. The real-time neutral atmospheric refraction models were refined by Lincoln Laboratory researchers David W. Blood and David Kwan in the early 1970s.

The early ionospheric refraction models addressed the fact that, in the ionosphere, the apparent target position is different for each operating frequency. Once implemented, the models removed frequency-dependent effects to enable all the RTS radars to produce more accurate, fused, position estimates. These position estimates, which are equivalent to the target's being detected in a vacuum, enabled an effective increase in the overall RTS detection sensitivity. The minimum target size that can be detected by radar is strongly dependent on its radar wavelength. The simultaneous application of integrated sensor systems at a broader spectrum of wavelengths enhances the span of their collective minimum detection sensitivity. The corrected position estimates also enable the radar systems to share target acquisition data (azimuth, elevation, and range) for real-time target tracking.

Theodore Pass implemented the real-time, two-frequency, simultaneous tracking method at ALTAIR utilizing UHF and VHF frequencies. The two-frequency method applies measurements of the difference in radar-to-target round-trip transit time for two signals at different frequencies, then leverages the dispersive propagation effects (cf. the Appleton-Hartree equation) to determine the ionospheric range delay and estimate the elevation-angle bias. This is the same method currently employed by the U.S. Air Force GPS to compute ionospheric corrections for dual-frequency receivers. The integration of the Roi-Namur radar systems enabled real-time ionospheric bias correction at TRADEX by leveraging the ionospheric parameters measured by ALTAIR.

These techniques satisfied RTS needs until the late 1970s when new space surveillance requirements for ALTAIR emerged to drive further tracking upgrades and refraction modeling. A significant difference between missile-reentry-vehicle data processing and space surveillance data processing is that reentry-vehicle data are generally post-processed to obtain maximum metric accuracy, while space surveillance data must be corrected in real time and immediately transmitted to the Joint Space Operations Center at Vandenberg Air Force Base in California. The majority of RTS space surveillance activities take place under low signal-to-noise-ratio (SNR) conditions while tracking deep-space satellites at single-frequency UHF (ALTAIR) or L band (TRADEX). In addition, in the late 1970s, the national need to compensate for transionospheric effects on RF systems (such as GPS) also drove ionospheric research to meet positioning-systems' performance requirements.

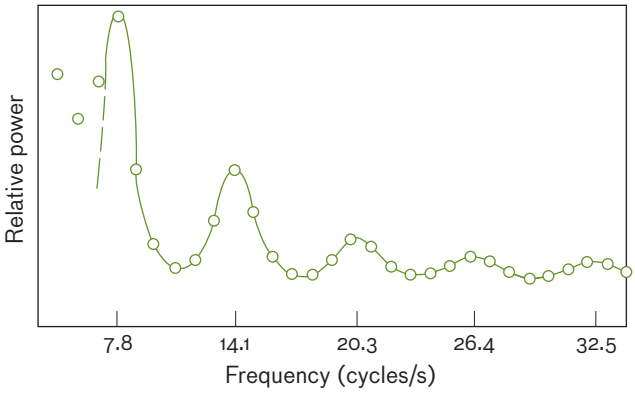

FIGURE 8. The chart shows the low-frequency resonance observed by Lincoln Laboratory personnel Balser and Wagner. This resonance was first proposed by Schumann in 1952.

During solar cycle 21 in 1980, the spatial and temporal variations of the equatorial ionosphere had significant impacts on the measurement accuracy of ALTAIR and TRADEX. Poorly modeled ionospheric range and elevation-angle biases were responsible for these impacts. The modeling required for ionospheric bias estimation is most challenging because RTS radar systems are located beneath one of the most complex regions of Earth's ionosphere.

During the late 1980s and early 1990s, complementary ionospheric modeling efforts took place at the Millstone Hill radar site in Westford, Massachusetts, (GPS Real-time Ionospheric Monitoring System [20]) and at RTS (first-order model, discussed later) for the purpose of single-frequency, ionospheric effects compensation at mid-latitude and at the equator. Both efforts explored the efficacy of exploiting GPS for real-time ionospheric position-bias correction.

As ALTAIR's single-frequency tracking requirements further expanded for space surveillance, a first-order vertical ionospheric range-delay model was added by Richard McSheehy from Lincoln Laboratory. This first-order model maintained a continuous estimate of the local iono-

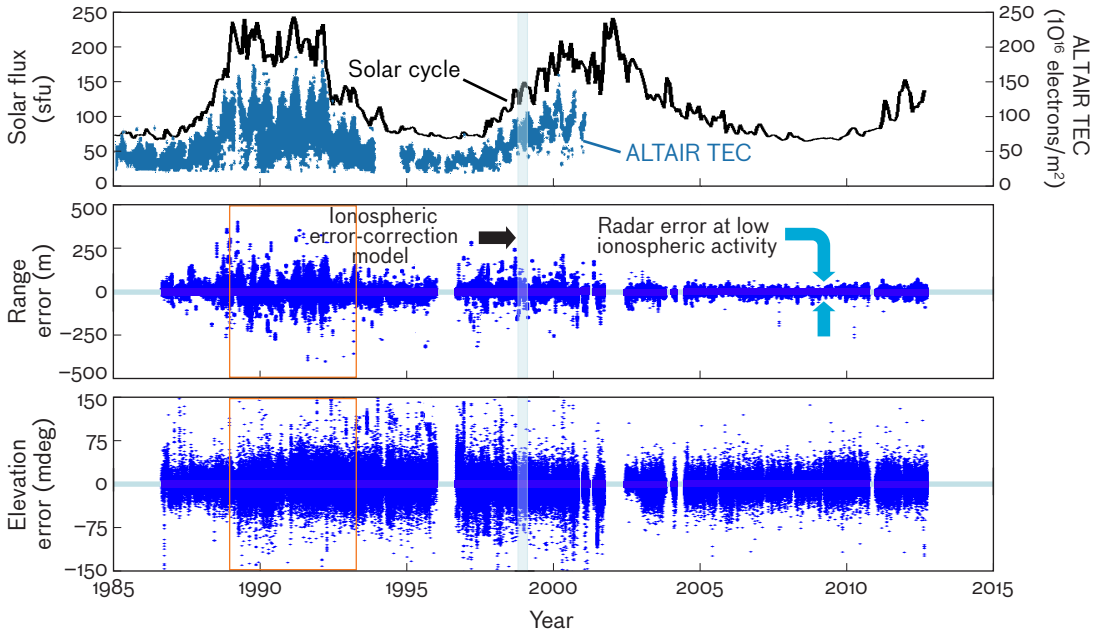

FIGURE 9. The three panels illustrate ALTAIR calibration errors caused by ionospheric effects. Note the large range-angle errors during 1989 to 1993.

sphere in the form of vertical ionospheric range delay; its goal was to support radar operation for extended periods without the assimilation of frequent ionospheric measurement updates. Vertical TEC data (one to four measurements) were collected daily by the ALTAIR system and assimilated by the first-order model. These updates scaled the first-order model to better match actual conditions.

In 1989, it became clear that the first-order model failed to meet the ALTAIR satellite-tracking accuracy requirements (Figure 9). The effects of increased solar activity were revealed by the examination of calibration data from the ALTAIR system. This modeling shortfall was evident and led to the development of the ionospheric error-correction model (IECM) that remains in use today.

The problem of collecting, calibrating, and assimilating GPS measurement data for real-time application was first solved by Anthea Coster and colleagues at the Millstone Hill radar facility, a mid-latitude facility. However, the distribution and dynamics of the mid-latitude ionosphere are less variable than the distribution and dynamics near the equator. Given the complex nature of the equatorial ionosphere and the existence of ubiquitous GPS data, it was recognized through a Small Business Innovative Research Project that the next model for RTS should contain a detailed physical model for equatorial ionospheric climatology, which is modified in real time by the assimilation of highly accurate GPS and ALTAIR TEC data [21]. The result is the IECM that combines a sophisticated climatological ionospheric model driven by real-time TEC measurements with the tropospheric correction model developed by Blood and Kwan.

The IECM capability resulted in a significant improvement in range data accuracy collected during ALTAIR's continuous, high-volume, satellite-tracking operation. The IECM has been operational at ALTAIR since spring 1998. Elevation-angle biases persist because of a lack of measurement data to provide electron-density structure along the propagation path (Figure 9). The continuing integration of existing RTS systems will greatly reduce this deficiency.

To summarize, a series of complementary characterization and modeling efforts evolved at RTS that included (1) ALTAIR real-time, two-frequency TEC measurements to compute radar corrections; (2) real-time TRADEX corrections using ALTAIR measurements; (3) ALTAIR first-order, single-frequency model; and (4) the assimilative climatology-based IECM, driven by highly calibrated real-time GPS data.

Research Experiments at RTS

Many scientists have used RTS in support of ionospheric research. Studies performed in the late 1970s and early

1980s include those by David Towle, Roland Tsunoda, and David Hysell. Towle from Lincoln Laboratory performed VHF and UHF backscatter radar studies of equatorial F region ionospheric irregularities and background densities in August 1977 and from July to August 1978 [22–25]. These measurements involved coordinated ground-based and in situ sensors. Plasma depletion regions were observed, consistent with predicted theoretical analysis. Tsunoda from Stanford Research Institute also performed studies on the growth of F region ionospheric irregularities and observed quasi-periodic variations that were mapped spatially over a 1200 km east-west distance by using incoherent scatter radar measurements. Hysell led a National Aeronautics and Space Administration (NASA) investigation into the electrodynamics of the post-sunset equatorial F region ionosphere. This research focused on further uncovering the emergence of spread F (signal distortion caused by the density irregularities in the F region ionosphere), as well as degradation of communication and navigation systems. Chemical release payloads on board sounding rockets were launched from Roi-Namur, and instrumented payloads measured in situ plasma density, temperature, collision frequency, electric fields, and neutral winds.

Starting in the 1990s, Keith Groves of the Air Force Research Laboratory led experiments to develop a radio scintillation nowcast and forecast capability (the Scintillation Network Decision Aid, SCINDA) to support DoD operational systems [26]. Measurements made with SCINDA at RTS are used in quasi-empirical models to characterize and predict the nighttime irregularities in the ionosphere. The predicted irregularities indicate the potential for intense amplitude and phase scintillations of satellite signals on frequencies from VHF to L band and for impacts on satellite communication, GPS navigation, and radar systems.

As a first step in the process of further integration of RTS ionospheric measurement systems, the IECM was upgraded in 2011 to support a greater data-recording capability. This increased capacity enables further ionospheric characterization and study of radar signal effects. The continuing integration of RTS systems is leading to a greater understanding of the physical properties of the ionosphere for an improved performance of national RF systems. ■

Acknowledgments

We greatly appreciate the assistance of Jeannine Ducharme from the Laboratory's archives for providing the historical record on Lincoln Laboratory ionospheric research. We also greatly appreciate and acknowledge the precision orbit error data used to assess radar tracking errors provided by Lori Thornton of the Space Situational Awareness Group.

REFERENCES

1. K.R. Roth, M.E. Austin, D.J. Frediani, G.H. Knittel, and A.V Mrstik, "The Kiernan Reentry Measurements System on Kwajalein Atoll," *Linc. Lab. J.*, vol. 2, no. 2, 1989, pp.247–276.
2. S.M. Hunt, S. Close, A.J. Coster, E. Stevens, L.M. Schuett, and A. Vardaro, "Equatorial Atmospheric and Ionospheric Modeling at Kwajalein Missile Range," *Linc. Lab. J.*, vol. 12, no. 1, 2000, pp. 45–64,
3. T.I. Gambosi, *Physics of the Space Environment.* Cambridge Atmospheric and Space Science Series. Cambridge, U.K.: Cambridge University Press, 1998.
4. M. Moldwin, *An Introduction to Space Weather.* New York: Cambridge University Press, 2008.
5. K. Davies, *Ionospheric Radio.* IET Electromagnetic Waves Series. London: Peter Peregrinus Ltd., 1990.
6. W.N. Hess, "The Effects of High Altitude Explosions," National Aeronautics and Space Administration Technical Note, TN D-2402, September 1964.
7. T.D. Carozzi, "Radio Waves in the Ionosphere: Propagation, Generation and Detection," Doctoral Thesis, Swedish Institute of Space Physics, IRF Scientific Report 272, August 2000.
8. R.J. Moffett, "The Equatorial Anomaly in the Electron Distribution of the Terrestrial F-Region," *Fundamentals of Cosmic Physics,* vol. 4, 1979, pp. 313–391.
9. G. Millman, *A Survey of Tropospheric, Ionospheric and Extraterrestrial Effects on Radio Propagation Between the Earth and Space Vehicles.* HMED Technical Publications, 1966.
10. G. Millman, "Ionospheric Electron Content Effects on Earth-Space Radio Propagation. A Review," General Electric Co. Syracuse, N.Y., Military Electronic Systems Operation, DTIC Access Number ADA096735, Dec. 1980.
11. T.H. Stix, *Waves in Plasmas.* New York: Springer-Verlag, 1992.
12. K. Bibl and B.W. Reinisch, "The Universal Digital Ionosonde," *Radio Science,* vol. 13, no. 3, 1978, pp. 519–530.
13. G. Williams, "Interpreting Digital Ionograms," *RadCom,* vol. 85, no.5, 2009, pp. 44–46.
14. W.O. Schumann, *Z. Naturforschung,* 7A, 149, 1952.
15. W.O. Schumann, *Z. Naturforschung,* 7A, 250, 1952.
16. M. Balser and C.A. Wagner, "Observations of Earth-Ionosphere Cavity Resonances," *Nature,* vol. 188, no. 4751, 1960, pp. 638–641.
17. B.J. Thompson, "Preserving IGY's History and Legacy," *Leading Edge,* vol. 26, no. 10, 2007, pp. 1296–1297.
18. D.T. Farley, "A Theory of Incoherent Scattering of Radio Waves by a Plasma 4. The Effect of Unequal Ion and Elec-

tron Temperatures," *Journal of Geophysical Research,* vol. 71, no. 17, 1966, pp. 4091–4098.
19. M.T. Rietveld, B. Isham, and I. Häggström, "Calibration of EISCAT Incoherent Scatter Radar Electron Densities and the Anomaly of 23–25 October 2003," EISCAT (European Incoherent Scatter) Scientific Association Report, v. 20071114, 2005.
20. A.J. Coster, E.M. Gaposchkin, and L.E. Thornton, "Real Time Monitoring System Using the GPS," Lexington, Mass.: MIT Lincoln Laboratory, Technical Report 954, 24 August 1992, DTIC Access Number AD-A256-916.
21. R.E. Daniel, "Parameterized Real-Time Ionospheric Specification Model (PRISM) 1.0," *Oceanography and Atmospheric Science,* Dec. 1991.
22. D.M. Towle, "VHF and UHF Radar Observations of Equatorial F Region Ionospheric Irregularities and Background Densities," *Radio Science,* vol. 15, no. 1, 1980, pp. 71–86.
23. R.T. Tsunoda, "Magnetic-Field-Aligned Characteristics of Plasma Bubbles in the Nighttime Equatorial Ionosphere," *Journal of Atmospheric and Terrestrial Physics,* vol. 42, no.8, 1980, pp. 743–752.
24. R.T. Tsunoda, "Time Evolution and Dynamics of Equatorial Backscatter Plumes. 1. Growth Phase," *Journal of Geophysical Research,* vol. 86, no. A1, 1981, pp. 139–149.
25. D.L. Hysell, M.F. Larsen, C.M. Swenson, A. Barjatya, T.F. Wheeler, M.F. Sarango, R.F. Woodman, and J.L. Chau, "Onset Conditions for Equatorial Spread-F Determined during EQUIS II," *Geophysical Research Letters,* vol. 32, no. 24, 2005, doi:10.1029/2005GL024743.
26. K.M. Groves, S. Basu, E.J. Weber, M. Smitham, H. Kuenzler, C.E. Valladares, R. Sheehan, E. MacKenzie, J.A. Secan, P. Ning, W.J. McNeill, D.W. Moonan, and M.J. Kendra, "Equatorial Scintillation and Systems Support," *Radio Science,* vol. 32, no. 5, 1997, pp. 2047–2064.

ABOUT THE AUTHORS

Stephen M. Hunt is a technical staff member in the Chemical and Biological Defense Systems Group. He joined Lincoln Laboratory's Aerospace Division at the Millstone Hill field site in 1988. He has served in the U.S. Army. He has a diverse technical background that has included roles as an analyst, principal investigator, and program manager. Technical areas he has worked in include space situational awareness, field systems and architectures, radar and electro-optical engineering, and defense techniques for weapons of mass destruction. He received a bachelor's degree in physics from Worcester Polytechnic Institute, a master's in astronomy, and a doctorate in computer and electrical engineering from Boston University.

Frederick J. Rich is a technical staff member in the Sensor Technology and System Applications Group. Since joining the Laboratory in 2008, he has worked on the NASA/NOAA Geostationary Operational Environmental Satellites-R program and ionospheric physics related to over-the-horizon radar. He previously worked at the Air Force Geophysics Laboratory as a scientist investigating the near-Earth space environment. He was involved with the space-weather sensors on the Defense Meteorological Satellite Program spacecraft. In his early career, he worked on the Apollo program at the Johnson Spacecraft Center. He received a bachelor's degree from Texas A&M University and a doctorate from Rice University.

Gregory P. Ginet is a senior staff member in the Space Systems Analysis Group. He came to Lincoln Laboratory in 2009 after more than 20 years at the Air Force Research Laboratory. He is currently involved in analyzing the effects of the space environment on radar and satellite systems, and in developing new models to specify and mitigate environmental effects to improve system performance. He is the principal investigator for the Wave-Particles Interaction Experiment on the Air Force's Demonstration and Science Experiment (DSX) satellite. He received a bachelor's degree and a doctorate degree in applied and engineering physics from Cornell University.